AMERICAN SOCIETY FOR MICROBIOLOGY | Infection and Immunity

Neuraminidase A-Exposed Galactose Promotes *Streptococcus pneumoniae* Biofilm Formation during Colonization

Krystle A. Blanchette,[a] Anukul T. Shenoy,[a,b] Jeffrey Milner II,[b] Ryan P. Gilley,[a] Erin McClure,[c] Cecilia A. Hinojosa,[a] Nikhil Kumar,[c] Sean C. Daugherty,[c] Luke J. Tallon,[c] Sandra Ott,[c] Samantha J. King,[d,e] Daniela M. Ferreira,[f] Stephen B. Gordon,[f] Hervé Tettelin,[c] Carlos J. Orihuela[a,b]

Department of Microbiology and Immunology, The University of Texas Health Science Center at San Antonio, San Antonio, Texas, USA[a]; Department of Microbiology, The University of Alabama at Birmingham, Birmingham, Alabama, USA[b]; Department of Microbiology and Immunology, Institute for Genome Sciences, University of Maryland School of Medicine, Baltimore, Maryland, USA[c]; Center for Microbial Pathogenesis, The Research Institute at Nationwide Children's Hospital, Columbus, Ohio, USA[d]; Department of Pediatrics, The Ohio State University, Columbus, Ohio, USA[e]; Department of Clinical Sciences, Liverpool School of Tropical Medicine, Liverpool, United Kingdom[f]

***Streptococcus pneumoniae* is an opportunistic pathogen that colonizes the nasopharynx. Herein we show that carbon availability is distinct between the nasopharynx and bloodstream of adult humans: glucose is absent from the nasopharynx, whereas galactose is abundant. We demonstrate that pneumococcal neuraminidase A (NanA), which cleaves terminal sialic acid residues from host glycoproteins, exposed galactose on the surface of septal epithelial cells, thereby increasing its availability during colonization. We observed that *S. pneumoniae* mutants deficient in NanA and β-galactosidase A (BgaA) failed to form biofilms *in vivo* despite normal biofilm-forming abilities *in vitro*. Subsequently, we observed that glucose, sucrose, and fructose were inhibitory for biofilm formation, whereas galactose, lactose, and low concentrations of sialic acid were permissive. Together these findings suggested that the genes involved in biofilm formation were under some form of carbon catabolite repression (CCR), a regulatory network in which genes involved in the uptake and metabolism of less-preferred sugars are silenced during growth with preferred sugars. Supporting this notion, we observed that a mutant deficient in pyruvate oxidase, which converts pyruvate to acetyl-phosphate under non-CCR-inducing growth conditions, was unable to form biofilms. Subsequent comparative transcriptome sequencing (RNA-seq) analyses of planktonic and biofilm-grown pneumococci showed that metabolic pathways involving the conversion of pyruvate to acetyl-phosphate and subsequently leading to fatty acid biosynthesis were consistently upregulated during diverse biofilm growth conditions. We conclude that carbon availability in the nasopharynx impacts pneumococcal biofilm formation *in vivo*. Additionally, biofilm formation involves metabolic pathways not previously appreciated to play an important role.**

Streptococcus pneumoniae (the pneumococcus) is a Gram-positive bacterium that can colonize the human nasopharynx. It is also an opportunistic pathogen capable of causing a wide spectrum of diseases, including sinusitis, otitis media, pneumonia, bacteremia, and meningitis (1). The greatest burden of pneumococcal disease is borne by infants, the elderly, and individuals who are immunocompromised (2, 3). Colonization of healthy individuals with the pneumococcus can last several months and is typically asymptomatic (1, 4, 5). It has been estimated that 25 to 40% of children in day care and 10 to 15% of adults with children are carriers of *S. pneumoniae* (6). Due to these high carriage rates, over 14.5 million episodes of invasive pneumococcal disease (IPD) are recorded annually in children worldwide (7, 8). Likewise, the pneumococcus is the leading cause of infectious death in the elderly, with a case-fatality rate of 10 to 25% (3, 9, 10). Since colonization is the first step in pneumococcal pathogenesis, understanding the underlying molecular mechanisms can potentially allow for design and development of new vaccines or drugs to prevent opportunistic infections in vulnerable individuals.

Biofilms are surface-attached communities of bacteria encased within an extracellular matrix (11, 12). Pneumococcal biofilms have been detected on nasal septum biopsy specimens from humans with sinusitis, on septal epithelia of experimentally challenged mice, and form *in vitro* on cultured respiratory epithelial cells and abiotic surfaces covered with bacterial media (13–17). Biofilm formation during colonization is thought to confer protection against host defenses and desiccation (18, 19). Dislodged pneumococcal aggregates in mucus may also act as vehicles for transmission on fomites (20). Of note, nutrient availability within the nasopharynx is thought to be poor, with carbohydrates and other essential metabolites limited in quantity or sequestered by the host (21). Along such lines, *in vitro* biofilm formation has been reported to be optimal during growth in nutrient-poor conditions (22), suggesting there may be a link between these occurrences.

The importance of carbohydrate acquisition for *S. pneumoniae* is evidenced by the fact that a large portion of its genome is de-

Received 5 April 2016 **Returned for modification** 21 May 2016
Accepted 21 July 2016

Accepted manuscript posted online 1 August 2016

Citation Blanchette KA, Shenoy AT, Milner J, II, Gilley RP, McClure E, Hinojosa CA, Kumar N, Daugherty SC, Tallon LJ, Ott S, King SJ, Ferreira DM, Gordon SB, Tettelin H, Orihuela CJ. 2016. Neuraminidase A-exposed galactose promotes *Streptococcus pneumoniae* biofilm formation during colonization. Infect Immun 84:2922–2932. doi:10.1128/IAI.00277-16.

Editor: A. Camilli, Tufts University School of Medicine

Address correspondence to Carlos J. Orihuela, corihuel@uab.edu.

K.A.B. and A.T.S. contributed equally to this article.

Supplemental material for this article may be found at http://dx.doi.org/10.1128/IAI.00277-16.

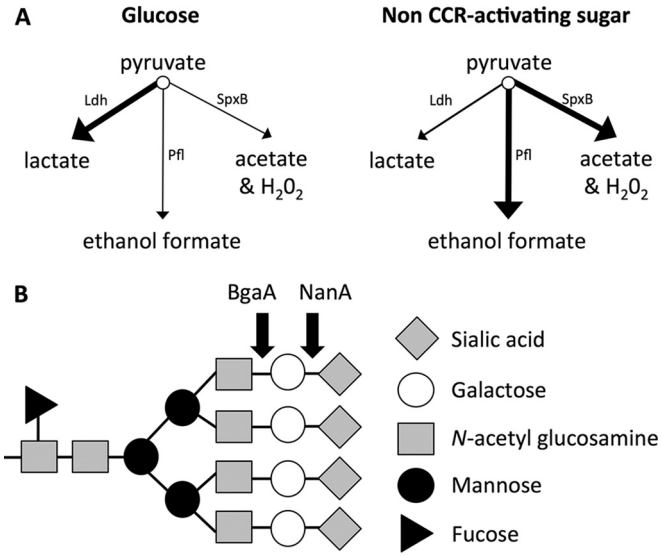

FIG 1 Pneumococcal metabolism and exoglycosidase activity. (A) Differential routes of *S. pneumoniae* pyruvate metabolism, with active pathways in the presence and absence of glucose-mediated CCR denoted with bold arrows. (B) Schematic representation of the exoglycosidase activity of the dominant pneumococcal neuraminidase A (NanA) and β-galactosidase A (BgaA), which cleave terminal sialic acid residues and β-1,4-linked galactose residues, respectively, off host glycoconjugates.

voted to carbohydrate uptake and processing (23). Similar to many other bacteria, the pneumococcus selectively metabolizes certain sugars first, such as glucose. When present, the pneumococcus modifies gene expression to ensure the prioritized usage of these sugars through a process called carbon catabolite repression (CCR). Pertinent to this article, glucose-mediated CCR results in the conversion of pyruvate to lactate, using the enzyme lactate dehydrogenase (24). Whereas in the absence of glucose and growth in galactose, pyruvate is converted to acetyl phosphate using the enzyme pyruvate oxidase (Fig. 1A) (25). Pyruvate oxidase is a key enzyme in the non-lactic acid-producing metabolic pathway in *S. pneumoniae*, and its homologues are under catabolite repression in a number of bacterial species. Encoded by *spxB*, pyruvate oxidase-dependent metabolism results in the conversion of pyruvate to acetyl-phosphate, which is a precursor for fatty acid biosynthesis and amino acids such as leucine (26, 27). During this process, hydrogen peroxide is generated, which has been shown to be a virulence determinant (28). Of note, we have previously documented a stark requirement for SpxB during *in vivo* biofilm formation (29); at the time, this was attributed to hydrogen peroxide-mediated bacterial autolysis, which was proposed to promote formation of extracellular matrix.

Numerous other pneumococcal genes have been shown to be required for successful colonization. This includes the gene encoding the dominant pneumococcal neuraminidase NanA, which cleaves terminal sialic acid residues off host glycoproteins (Fig. 1B) (30–32). NanA has been proposed to promote colonization by multiple means: (i) NanA frees sialic acid, which then serves as carbon source for pneumococci in the nasopharynx (33), (ii) NanA exposes galactose and *N*-acetylglucosamine residues normally shielded by sialic acid for bacterial adhesion (34), (iii) NanA allows the pneumococcus to escape entrapment within the heavily glycosylated mucus (35, 36), and (iv) NanA cleaves glyconjugates off host immune effector proteins, altering their function (37). Of note, a *nanA*-deficient mutant of *S. pneumoniae* was reported to have decreased biofilm formation during growth on cultured epithelial cells *in vitro* (30).

Herein, we examined the requirement for galactose, the predominant sugar found in the nasopharynx, for biofilm formation during colonization and the role of neuraminidase A in its exposure on the cell surface. We also use transcriptome sequencing (RNA-seq) to characterize the *S. pneumoniae* transcriptome during planktonic and biofilm growth on distinct carbon sources. Our findings suggest that anatomical site-specific carbon availability impacts the growth phenotype of *S. pneumoniae in vivo*.

MATERIALS AND METHODS

Human samples. Nasal lavage fluid (NALF) and serum samples were collected from human volunteers experimentally colonized with *S. pneumoniae* serotype 6B strain BHN418 as part of independent studies (38, 39). Briefly, healthy adult volunteers 18 to 60 years of age were inoculated with pneumococcus as previously described (40). Samples were collected at day 21 following inoculation and frozen, with designations made as to whether individuals were colonized or not based on successful culture of *S. pneumoniae* from NALF. Samples were provided in a deidentified fashion and deemed by the Institutional Review Board at The University of Texas Health Science Center at San Antonio (UTHSCSA) as not meeting the criteria for human subject research.

Mice. Female BALB/c mice 6 weeks of age were obtained from The Jackson Laboratory (Bar Harbor, ME). All animal experiments were performed with protocols reviewed and approved by the Institutional Animal Care and Use Committees at UTHSCSA (protocol no. 13032-34-01C). Animal care and experimental protocols adhered to Public Law 89-544 (Animal Welfare Act) and its amendments, Public Health Services guidelines, and the *Guide for the Care and Use of Laboratory Animals* (41).

Bacteria. Mouse colonization studies were performed using serotype 6A strain 6A-10 or isogenic mutants deficient in neuraminidase A (i.e., 6A-10 Δ*nanA*), β-galactosidase A (i.e., 6A-10 Δ*bgaA*), or pyruvate oxidase (i.e., 6A-10 Δ*spxB*). 6A-10 has previously been shown to form robust biofilms *in vivo* (29). Laboratory strains D39 and TIGR4, along with a TIGR4 mutant deficient in SpxB (i.e., T4 Δ*spxB*), were used for the testing of biofilm formation *in vitro* (23, 42). Isogenic deletion mutants were created by allelic exchange using mutagenic PCR constructs consisting of fragments of the flanking genes around an erythromycin resistance cassette (43). Unless noted otherwise, *S. pneumoniae* cells were grown in Todd-Hewitt broth (THB) at 37°C in 5% CO_2. Mutants were kept under antibiotic selection with 1 μg/ml erythromycin at all times with the exception of outgrowth for experiments. In these instances, antibiotics were removed to avoid confounding effects of the antimicrobial on autolysis (44), which is known to affect biofilm formation (22).

Measurement of carbohydrate levels in human nasal lavage fluid and serum. The concentration of free glucose, galactose, and sialic acid were measured using fluorescent carbohydrate detection kits from BioVision (Milpitas, CA).

Staining of septal epithelium to visualize exposed galactose. Female 6-week-old BALB/c mice were inoculated with 10^5 CFU of 6A-10 in 10 μl saline as previously described (29). Septa were collected 7 days postinoculation (dpi) without removal from the nasal cavity (45). Samples were placed in 10% neutral buffered formalin overnight and then transferred to 15% EDTA for decalcification for 4 weeks, with weekly changes of EDTA. Following decalcification, samples were frozen in optimal cutting temperature compound and cryo-sectioned. Slides were stained with fluorescein isothiocyanate (FITC)-labeled *Erythrina cristagalli* lectin (Vector Laboratories, Burlingame, CA) for 30 min at room temperature. Following routine staining with DAPI (4′,6-diamidino-2-phenylindole), slides were visualized using a Prairie Ultima 2-photon confocal microscope system (Bruker, Middleton, WI).

Visualization of *in vivo* biofilms by SEM. Nasal septa from colonized mice were collected as described above, except the mice were exsanguinated and then perfused with saline following euthanasia to prevent the accumulation of erythrocytes during dissection procedures. Nasal septa were prepared for scanning electron microscopy (SEM) as described previously (29).

***In vitro* biofilm formation.** Biofilms were grown with THB in Costar 6-well polystyrene plates (Corning) (29). Medium was changed after 24 h, and biofilm biomass was measured after 48 h. To determine biofilm biomass, wells were stained with 1% crystal violet for 10 min. Following three rinses with saline, biofilm-attached crystal violet stain was solubilized using 95% ethanol, and the optical density at 540 nm was read using a HybridH4 plate reader (BioTek, Winooski, VT). For experiments using sugar-supplemented media, the designated sugar was added in increasing concentrations to 50% THB prior to its use and filter sterilized. In other instances, acetate and lactate at the designated concentrations were added to media, and the pH of the medium was adjusted to 7.4 before experimental use.

Adhesion assay. Detroit 562 nasopharyngeal epithelial cells were grown to confluence in 24-well plates in F-12 medium supplemented with 10% fetal bovine serum. Tumor necrosis factor alpha was added to each well to a final concentration of 10 ng/ml, and plates were incubated at 37°C for 2 h. Cells were washed, 1 ml of F-12 medium containing 10^6 CFU of *S. pneumoniae* was added, and the mixture was incubated for 1 h at 37°C. Cells were washed with sterile saline three times and scraped into 100 μl water, and lysates were plated to determine the number of adherent pneumococci. Experiments were performed in four biological replicates with three technical replicates each time.

Isolation of RNA. *S. pneumoniae* was grown planktonically or in polystyrene 6-well plates as 2-day-old biofilms in 50% THB supplemented with the designated sugar at 1%. Planktonic pneumococci were pelleted by centrifugation, washed with saline, treated with RNAprotect (Qiagen), and stored at −80°C. Pneumococci in biofilms were rinsed with saline, scraped off the plastic surface, pelleted, treated with RNAprotect, and stored at −80°C. Samples for each of the 5 growth conditions were collected in triplicate (15 samples total). Total RNA was extracted from each replicate separately using enzymatic lysis of pneumococcal cells (10 μl mutanolysin, 20 μl proteinase K, 15 μl lysozyme, and 55 μl Tris-EDTA [TE]) followed by RNA extraction with the RNeasy Micro kit (Qiagen) with DNase treatment on column and in solution. Samples were then depleted of rRNAs using the Ribo-Zero rRNA removal kit for Gram-positive bacteria (Illumina, San Diego, CA).

RNA-seq. Illumina strand-specific RNA-seq libraries were constructed with the TruSeq RNA sample prep kit (Illumina, San Diego, CA) per the manufacturer's protocol. Between 1st and 2nd strand cDNA synthesis, the primers and nucleotides were removed from the samples with NucAway spin columns (Ambion, Austin, TX). The 2nd strand was synthesized with a deoxynucleoside triphosphate (dNTP) mixture containing dUTP. Adapters containing 6 nucleotide indexes were ligated to the double-stranded cDNA. After adapter ligation, the 2nd strand cDNA was digested with 2 U of uracil-*N*-glycosylase (Applied Biosystems, Carlsbad, CA). Size selection of the library was performed with AMPure XT beads (Beckman Coulter Genomics, Danvers, MA). All 15 libraries were multiplexed on one flow cell lane of a 150-nucleotide (nt) paired-end run of the Illumina HiSeq4000 sequencing platform.

Transcriptomic analyses. Reads from each of the 15 samples were mapped onto the newly sequenced *S. pneumoniae* 6A-10 genome using Bowtie version 0.12.9 (46). The 6A-10 genome was sequenced using the Pacific Biosciences RS-II platform and assembled into a single contig. The alignment BAM files from Bowtie were used to compute gene expression levels and test each gene for differential expression. The number of reads that mapped to each 6A-10 gene was calculated using the Python package HTSeq version 0.4.7 (47). The read count represents the expression of the gene. Differential gene expression analysis was conducted using the DESeq R package version 1.5.24 (available from Bioconductor [48]). The DESeq analysis resulted in the determination of potential differentially expressed genes compared between the control planktonic samples and the biofilm samples. The read counts for each sample were normalized for sequencing depth and distortion caused by highly differentially expressed genes. Then the negative binomial model was used to test the significance of differential expression between two conditions. The differentially expressed genes were deemed significant if the false discovery rate was less than 0.05 and the gene expression was above the 10th percentile and showed greater than a 2-fold change difference (upregulated or downregulated) between the conditions. Finally, because no metabolic pathway information exists in the public domain for the newly sequenced 6A-10 genome, TIGR4 orthologs of 6A-10 differentially regulated genes were subjected to a pathway enrichment analysis with GAGE version 2.18.0 (49) and KEGG orthology terms and pathway maps for *S. pneumoniae* TIGR4 (50). The pathway analysis output was filtered to include only nonredundant pathways at $P < 0.05$. Heat maps were generated with the R package gplots version 2.17.0. Differentially regulated genes involved in pyruvate metabolism in *S. pneumoniae* were painted on the KEGG pyruvate metabolism reference pathway (SPN00620) using the packages GAGE and Pathview (49, 51).

Statistical analyses. Statistical analyses of non-*in silico* data were performed using Prism 5.0 (GraphPad Software, La Jolla, CA). All nonparametric data sets were analyzed using a Mann-Whitney test, while parametric data sets were analyzed using Student's *t* test. One-way analysis of variance (ANOVA) was used for multiple group analyses. *P* values of <0.05 were deemed significant.

Nucleotide sequence accession number. RNA-seq reads were deposited at the Gene Expression Omnibus (GEO) database under accession number GSE85196.

RESULTS

Glucose, sialic acid, and galactose levels vary in an anatomical site-specific manner. We first sought to determine the abundance of CCR-inducing glucose and the less preferred carbohydrates sialic acid and galactose at two anatomical sites important for pneumococcal infection: the nasopharynx and within the blood. To do this, we tested paired NALF and serum samples taken from experimentally colonized human adult volunteers 21 days after inoculation with *S. pneumoniae* strain BHN418, a serotype 6B isolate (38, 39). Paired samples from carriage-negative individuals were also tested for control. Glucose was by far the most abundant sugar present within serum (90.23 ± 11.33 nmol/ml), with sialic acid present at modest concentrations (60.66 ± 3.31 nmol/ml) and galactose at low levels (10.76 ± 0.46 nmol/ml). In contrast, glucose was undetectable, sialic acid levels were significantly lower (20.88 ± 1.01 nmol/ml), and galactose emerged as the most abundant sugar (37.09 ± 0.89 nmol/ml) in NALF samples (Fig. 2A). Significant differences in the levels of all three carbohydrates were observed between NALF and serum samples. Yet only galactose levels were significantly different between NALF from carriage-positive individuals versus carriage-negative controls (carriage positive, 39.39 ± 0.646 nmol/ml; carriage negative, 34.80 ± 1.12 nmol/ml; $P = 0.0087$). This modest increase in NALF galactose levels suggested colonizing pneumococci perhaps liberated this sugar. As such, we examined nasal septa taken from colonized and uncolonized mice 7 days postinoculation (dpi) with strain 6A-10, a serotype 6A nasopharyngeal isolate of *S. pneumoniae* (Fig. 2B) (29). Mice carrying 6A-10 exhibited a high degree of exposed galactose on septal epithelial cells as determined by fluorescent staining with an FITC-labeled lectin specific for this sugar. Lectin staining was not evident in septa from uninfected controls and was strongly diminished in septa from mice experimentally colonized with 6A-10 Δ*nanA*, an isogenic mutant deficient in NanA. Thus,

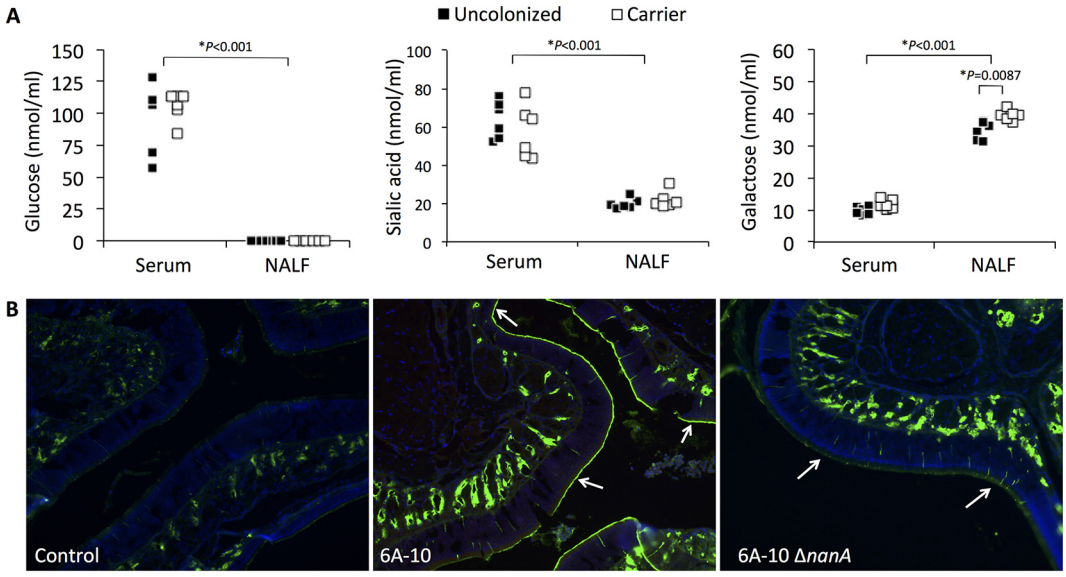

FIG 2 Galactose is present in the nasopharynx, and its exposure is increased following colonization with *S. pneumoniae*. (A) Relative levels of sugars present in serum and NALF of patients experimentally colonized with *S. pneumoniae* strain BHN418 (white squares) versus carriage-negative controls (black squares). Each square represents an individual clinical sample. Statistical analyses were done using the Mann-Whitney test. *P* values of ≤0.05 were considered statistically significant. Asterisks indicate specific *P* values. (B) Representative fluorescence microscopy images of sections obtained from septa of mice colonized with 6A-10, 6A-10 Δ*nanA*, or a mock-treated control ($n = 3$ per cohort). Labeling was performed using FITC-labeled *E. cristagalli* lectin to indicate the presence of exposed galactose (green) and DAPI (blue) to visualize cells. Exposed galactose present on the apical mucosal epithelial cell layer is denoted by white arrows.

exposure of galactose on epithelial cells required neuraminidase activity by the colonizing strain.

Neuraminidase A and β-galactosidase A activities are required for biofilm formation within the nasopharynx. We have previously reported that biofilms form within the nasopharynx of *S. pneumoniae*-colonized mice (29). Consistent with this report, we observed 6A-10 biofilms formed on nasal septa epithelial cells of mice at 7 dpi using SEM (Fig. 3). In stark contrast, septa from mice colonized with 6A-10 Δ*nanA* appeared identical to phosphate-buffered saline (PBS)-treated animals, with the exception of the presence of leukocytes. In a similar fashion, mice inoculated with 6A-10 Δ*bgaA*, an isogenic mutant deficient in β-galactosidase A, also failed to develop bacterial biofilms on nasal septa epithelial cells at 7 dpi (Fig. 3). Briefly, BgaA is capable of cleaving β1-4-linked galactose that underlies terminal sialic acid on host glyconjugates (Fig. 1B). Importantly, the numbers of pneumococci present in NALF as measured by colony counts were not significantly different between 6A-10-, 6A-10 Δ*nanA*-, or 6A-10 Δ*bgaA*-colonized mice at 7 and 14 dpi, albeit there was a trend toward reduced 6A-10 Δ*bgaA* levels on day 7 in NALF (see Fig. S1 in the supplemental material). These results show that NanA and BgaA impact the growth phenotype of the pneumococcus during asymptomatic colonization, although they have no obvious impact on isolated NALF bacterial counts.

Neuraminidase A and β-galactosidase A are not required for *in vitro* biofilm formation and have differential contributions to adhesion. One possible explanation for the lack of *S. pneumoniae* biofilms formed on the septa of 6A-10 Δ*nanA*- and 6A-10 Δ*bgaA*-colonized mice was that these encoded enzymes modulate the interactions between individual pneumococci. Suggesting otherwise, we observed no differences between 6A-10, 6A-10 Δ*nanA*, or 6A-10 Δ*bgaA* during *in vitro* biofilm formation on polystyrene plates (Fig. 4A). Alternatively, these enzymes may promote bacterial adhesion to epithelial cells, a key first step for biofilm formation. Herein, we observed no significant attenuation in the adhesion of encapsulated 6A-10 Δ*nanA* to Detroit 562 epithelial cells *in vitro* (Fig. 4B). However, we did observe that 6A-10 Δ*bgaA* was less adhesive than its wild-type parent strain. Thus, the attenuation of 6A-10 Δ*bgaA*, but not 6A-10 Δ*nanA*, with regard to *in vivo S. pneumoniae* biofilm formation may be due to decreased adhesion to host cells.

Non-CCR-acting carbohydrates are permissive for biofilm formation. We subsequently tested if reliance on specific carbohydrates impacted the ability of *S. pneumoniae* to form biofilms *in vitro*. To do this, we used 50% THB medium that contained 0.1% glucose as the base medium. We used 50% THB because it permitted detection of positive and negative changes in biofilm biomass during growth of pneumococci *in vitro* with different carbon sources (see Fig. S2A in the supplemental material). Moreover, because once medium was supplemented with other carbohydrates, with the exception of high levels of sialic acid, no detrimental effect on growth was detected (see Fig. S2B and C). Supplementation of 50% THB medium with CCR-inducing glucose, sucrose, and fructose was inhibitory to biofilm formation *in vitro*. In contrast, the less preferred sugars galactose and lactose were permissive for *in vitro* biofilm formation (Fig. 5A). Sialic acid was permissive for biofilm formation but only at low concentrations (Fig. 5A). Higher concentrations (>0.125%) of sialic acid were toxic to 6A-10 (see Fig. S2B), precluding its study. Importantly, the inhibitory effects of glucose on *in vitro* biofilm formation were also observed in laboratory strains TIGR4 and D39 (see Fig. S3 in the supplemental material). We also observed that deletion of *spxB*, which is repressed during glucose-induced CCR, in 6A-10 and TIGR4 backgrounds resulted in mutants unable to form biofilms *in vitro* (Fig. 5B). What is more, addition of acetate to the culture medium increased the biomass of 6A-10 biofilms. In contrast,

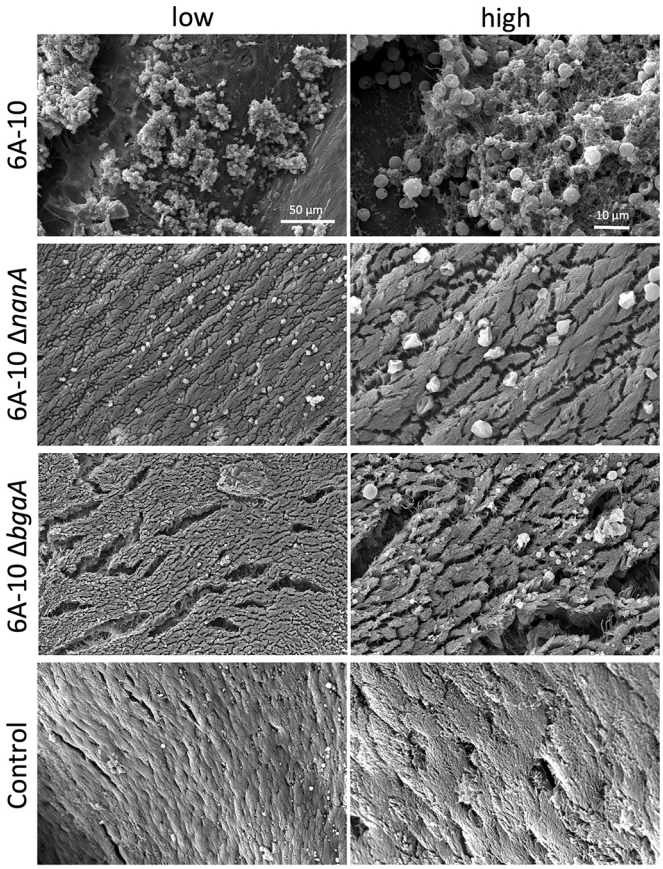

FIG 3 Neuraminidase A and β-galactosidase A contribute to robust biofilm formation within the nasopharynx. Shown are representative scanning electron microscopy images (at low and high magnification) of nasal septal epithelia isolated from mice colonized with wild-type *S. pneumoniae* strain 6A-10, 6A-10Δ*nanA*, or 6A-10 Δ*bgaA*. A minimum of 5 septa were examined per cohort. Nasal septa of mice challenged with saline were used as negative controls. Septa were collected at 7 dpi.

addition of lactate caused a downward trend in 6A-10 biofilm biomass (Fig. 5C). We conclude that biofilm formation is tied to a non-lactic acid-producing (i.e., less preferred) carbohydrate-driven metabolism.

Metabolic pathways differentially regulated during biofilm formation. To elucidate other metabolic pathways that might be involved in biofilm formation, we performed RNA-seq using RNA isolated from 6A-10 grown planktonically and as a biofilm in 50% THB and in 50% THB supplemented with 1% galactose. We also performed RNA-seq on 6A-10 RNA isolated from pneumococci grown planktonically in 50% THB supplemented with 1% glucose. 6A-10 does not form biofilms in medium supplemented with glucose (Fig. 5A): as such, this growth condition was not included in these analyses. TIGR4 orthologs of 6A-10 genes determined to be differentially expressed in biofilm versus planktonic growth across the different conditions by DESeq analysis of RNA-seq data were subjected to a pathway enrichment analysis performed with GAGE, KEGG orthology terms, and pathway maps for *S. pneumoniae* TIGR4 (Fig. 6A). We observed that the genes involved in pyruvate metabolism (KEGG pathway spn00620) were upregulated across all of our comparisons (Fig. 6A). In addition, genes involved in fatty acid biosynthesis (KEGG pathway spn00061) and fatty acid metabolism (KEGG pathway spn01212) were also consistently upregulated. Genes involved in pyrimidine metabolism (KEGG pathway spn00240) were only upregulated when comparisons were made against planktonic pneumococci grown in THB supplemented with a sugar. Likewise, genes involved in ribosome expression (KEGG pathway spn03010) were exclusively upregulated in all instances when biofilm pneumococci were grown in unsupplemented medium. These latter two pathways may be regulated as a result of metabolite-specific phenomena. Genes involved in oxidative phosphorylation (KEGG pathway spn00190) were downregulated, but this too was only observed when comparisons were made with biofilm pneumococci grown in supplemented medium. It is of note that the pyruvate metabolism pathway ties directly into fatty acid synthesis and the fatty acid metabolism pathway (Fig. 6B). As such, these analyses suggest that fatty acid biosynthesis is an important aspect of pneumococcal biofilm formation that was up to this point unappreciated.

Of note, *bgaA* expression was modestly increased under all growth conditions when medium was supplemented with galactose versus expression in unsupplemented medium. It was also increased in galactose planktonic versus glucose planktonic cultures. No such differences were observed for *nanA*. In contrast,

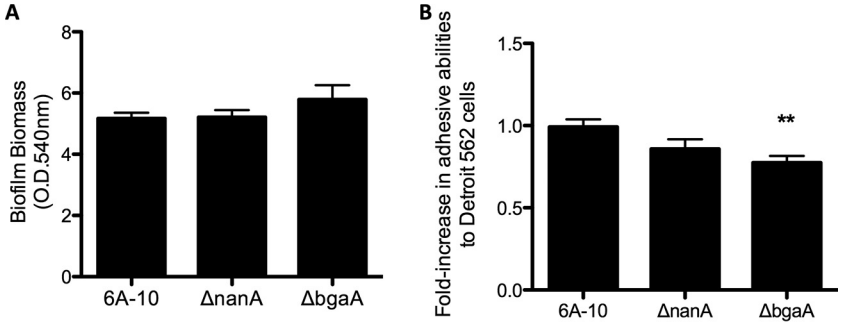

FIG 4 Contribution of neuraminidase A and β-galactosidase A to biofilm formation and adhesion to host cells *in vitro*. (A) Biofilm-forming ability of strains 6A-10, 6A-10 Δ*nanA*, and 6A-10 Δ*bgaA* in a 48-h 6-well polystyrene plate model. Biofilm biomass was measured using the amount of crystal violet trapped within the biofilm at 540 nm. (B) Abilities of strains 6A-10, 6A-10 Δ*nanA*, and 6A-10 Δ*bgaA* to adhere to Detroit 562 cells as measured by recoverable CFU following washing and plating of bacteria. Values are expressed as fold increase in adhesion relative to wild-type strain 6A-10. Statistical analysis was performed using the Mann-Whitney test. **, $P \leq 0.01$. Experiments were repeated three times. Mean results are shown, and error bars represent the standard error of the mean.

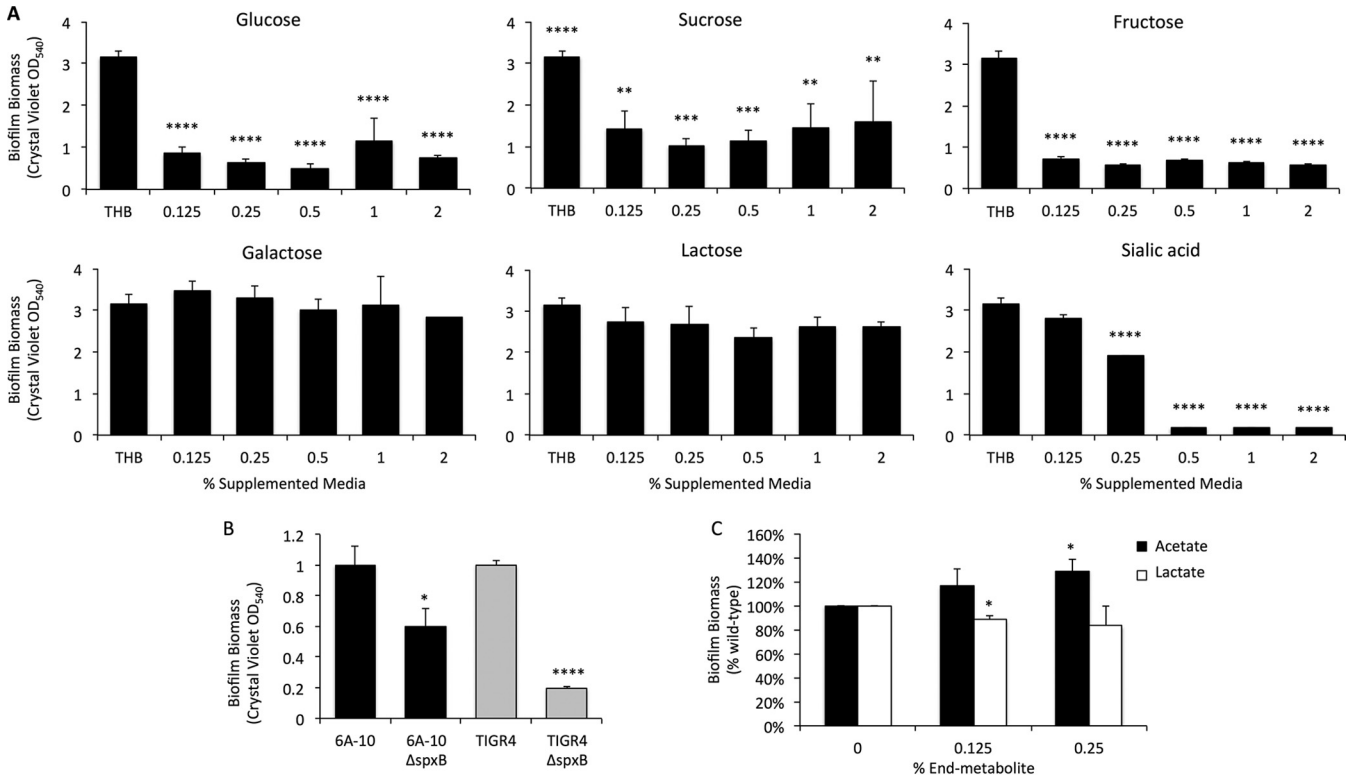

FIG 5 Non-CCR-acting carbohydrates are permissive for biofilm formation. (A) Pneumococcal biofilm formation was assessed in diluted medium (50% THB) supplemented with increasing concentrations of glucose, sucrose, fructose, galactose, lactose, and sialic acid in a 48-h 6-well polystyrene plate model. Statistical analysis was performed using one-way ANOVA. Statistical significance was calculated by comparing the biofilm biomass of supplemented media with that of unsupplemented sugar-free media. (B) Biofilm biomass at 48 h by the wild-type TIGR4 and 6A-10 strains and their respective *spxB* mutants. Statistical analyses compared the mutant to its wild-type counterpart using Student's *t* test. (C) Biofilm biomass by strain 6A-10 in the presence of different concentrations of the end metabolites acetate (black bars) and lactate (white bars). Statistical analyses were performed by comparing the biofilms in supplemented media with those in unsupplemented medium using Student's *t* test. *, $P \leq 0.05$; **, $P \leq 0.01$; ***, $P \leq 0.001$; ***, $P \leq 0.0001$. Experiments were repeated a minimum of three times. Mean results are shown, and error bars represent the standard error of the mean.

nanA expression was reduced during biofilm growth in galactose versus unsupplemented 50% THB (see Fig. S4 in the supplemental material).

DISCUSSION

Carbon acquisition is critical for *S. pneumoniae* survival. For this reason, a major part of the pneumococcus genome is dedicated toward the uptake and processing of carbohydrates, including sialic acid, galactose, and glucose (23, 52). Since the initial discovery that the pneumococcus produces neuraminidase, much effort has gone toward elucidating its role in the disease process (30, 34, 35, 53, 54), determining the impact of free sialic acid on the bacterium's metabolism (31, 33, 55, 56), and testing whether inhibition of neuraminidase activity is protective (57). Along such lines, Marion et al. determined that *S. pneumoniae* was capable of growth with sialic acid as the sole carbon source (33). Similar to our findings, it was reported that growth was slower and the cultures failed to reach the same optical density observed when glucose was used instead as the sole carbon source. Subsequently, Trappetti et al. showed that exogenous sialic acid enhanced biofilm formation *in vitro* (31). Herein, we build on these observations and suggest that one primary role for pneumococcal NanA is to facilitate exposure of underlying galactose residues and that the predominance of this less-preferred carbon within the nasopharynx, along with the absence of glucose, promotes growth of *S. pneumoniae* in a biofilm.

There have been multiple reports that examined a role for NanA and BgaA in adhesion to epithelial cells. Tong et al. showed that serotype 2 strain D39 deficient in NanA was attenuated for adherence to chinchilla tracheal epithelium and colonization *in vivo* (34, 58). Brittan et al. also reported that a D39 NanA-deficient mutant was attenuated for its ability to adhere to the pharyngeal, laryngeal, and lung epithelial cells (59). However, King et al. reported no differences in adhesion of D39 Δ*nanA* to cells of Detroit 562 human upper airway epithelial lines (36). These discrepancies might be attributed to differences in experimental procedures used and intrinsic variability in the D39 stocks that were tested. Nonetheless, King et al. showed that an unencapsulated derivative of D39 lacking either NanA or BgaA (i.e., R6 Δ*nanA* or R6 Δ*bgaA*) had reduced adhesive abilities in comparison to wild-type R6, a finding that suggested a more obvious role for these proteins in adhesion when in an unencapsulated setting (36). In a later study, Limoli et al. showed that the role of BgaA in promoting adhesion extended to D39 and C06_18, a serotype 22F strain, but not another two strains belonging to other serotypes (60). Of note, surface accessibility of pneumococcal adhesins has since been shown to depend on capsule type, with differences reported across isogenic capsule switch mutants having the same genome (61). Thus,

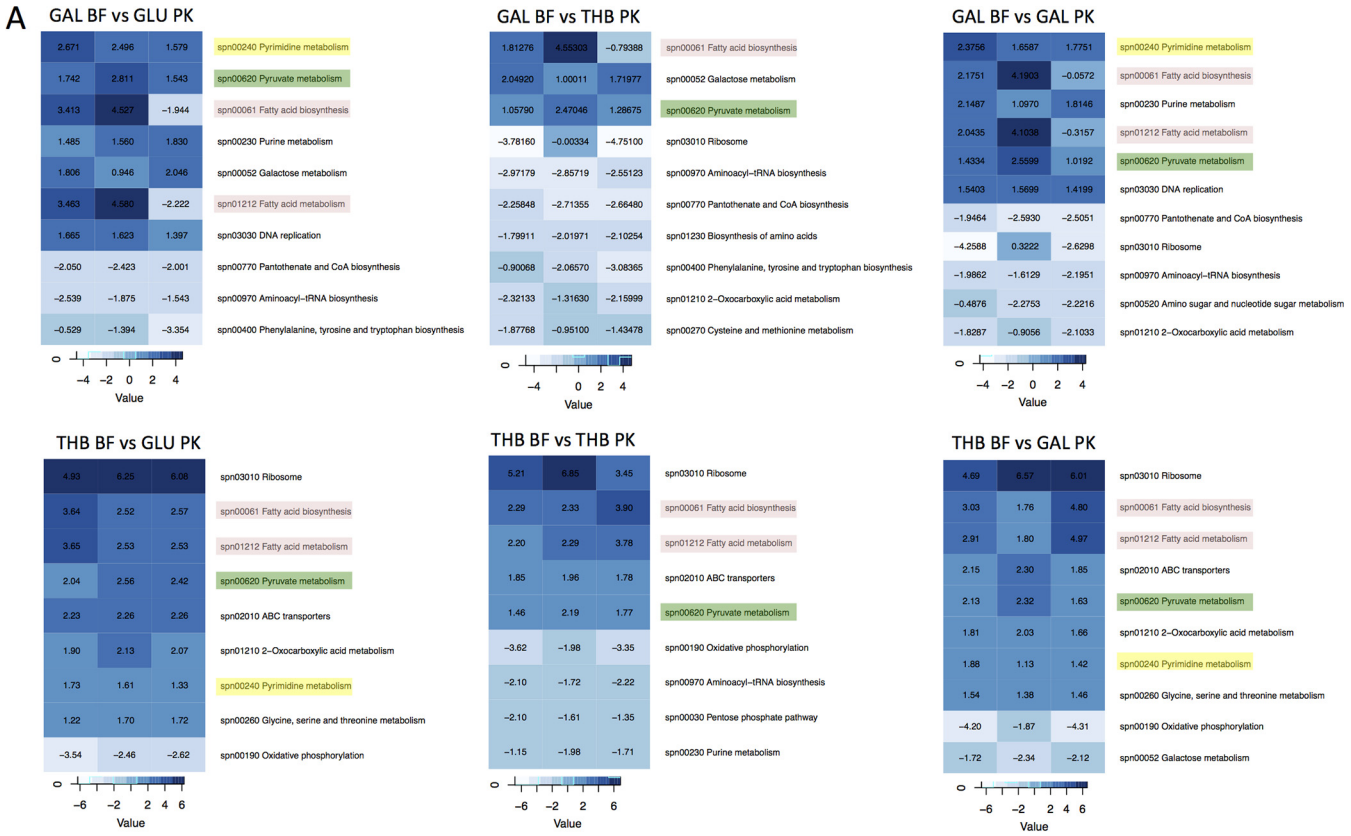

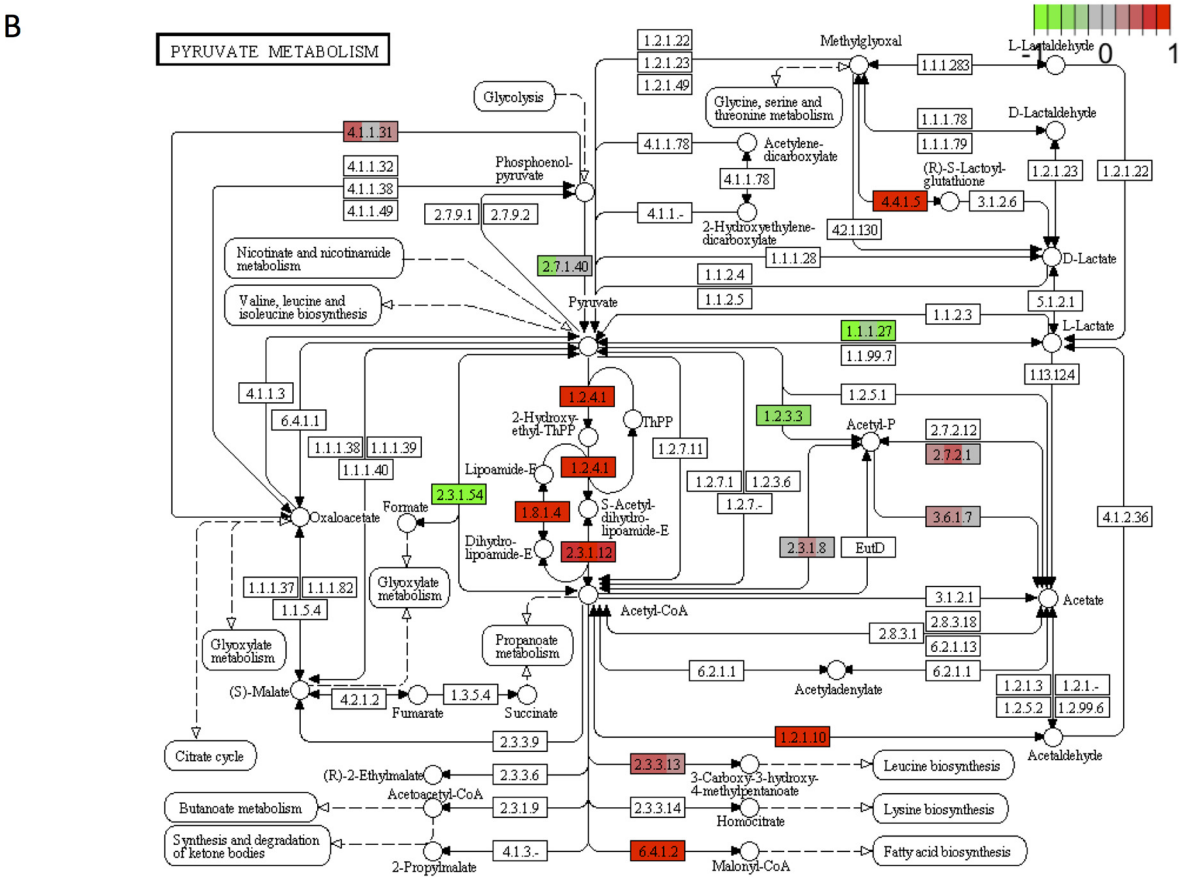

the different capsule types of the strains tested are a plausible explanation for the differences observed by Limoli et al. (60).

Our SEM data make it clearly evident that pneumococcal neuraminidase A and β-galactosidase A activities were essential for the formation of 6A-10 biofilm aggregates on nasal septa of infected mice. This was despite there being no discernible effect of deletion of these genes on biofilm formation *in vitro*. For this reason, the role of NanA and BgaA in the formation of biofilms *in vivo* most likely involves a host component, which we propose is cell surface galactose that underlies sialic acid. In support of this, we demonstrate that the presence of NanA dramatically increased the exposure of non-CCR-acting galactose on the surface of septal epithelial cells *in vivo*. Moreover, that *spxB* gene, whose expression is suppressed by glucose-mediated CCR and derepressed under growth in galactose (26, 27), was essential for biofilm formation *in vitro* and *in vivo*. The latter *in vivo* result was recently published by our group (29). Consistent with this notion, we detected galactose and not glucose in NALF samples obtained from colonized individuals. Thus, the pneumococcus operates in the absence of glucose-mediated CCR during asymptomatic colonization, and growth under less-preferred alternate carbon sources, such as galactose, is permissive for biofilm growth. Of note, the discrepancy between the *in vitro* and *in vivo* requirements for NanA and BgaA in biofilm formation highlights the necessity of animal testing to discern the full contribution of suspected virulence determinants.

It is of note that the absence of NanA or BgaA in colonizing 6A-10 did not have a negative impact on *S. pneumoniae* titers recovered from NALF. One caveat to this is that we did not examine septal homogenates for bacterial burden (i.e., intimately attached pneumococci were not counted); this was because our approach was longitudinal in the same set of mice. Thus, it is possible that overall burdens were different. Nonetheless, the sustained presence of pneumococci in NALF indicates that biofilm formation is not requisite for survival within the nasopharynx and that planktonic pneumococci are able to evade host clearance. This also implies that biofilm aggregates may play a different role—perhaps resistance to desiccation during transmission on fomites (20). It also suggests that the pneumococcus is able to obtain sufficient nutrients despite the absence of these enzymes. Even so, the observations that biofilms form in the nasopharynx and that biofilm formation is impaired by glucose and other CCR-inducing sugars suggest that biofilms are in some manner beneficial to the bacterium and that carbon availability is a key environmental factor underlying biofilm formation.

Over the past several years, we and other investigators have explored the role of pneumococcal biofilms in the nasopharynx as a mechanism for persistence and transmission. The most unexpected finding has been that pneumococci within biofilms are less virulent than their planktonic counterparts. As evidence for this, we and others have shown that biofilm pneumococci have reduced production of capsular polysaccharide and pneumolysin, are hyperadhesive yet have an inability to invade epithelial cells, and elicit a muted inflammatory response from host cells (29, 62, 63). Most recently Marks et al. demonstrated that inflammatory host signals, including the addition of glucose, resulted in the dispersal of *S. pneumoniae* biofilms. Furthermore, these biofilm-dispersed pneumococci were hypervirulent (62). Therefore, the absence of glucose in the nasopharynx of colonized adults may help to explain why colonization does not typically result in an overt inflammatory state. Additionally, increases in glucose concentration within the nasopharynx—for example, as a result of virus-induced inflammation or even uncontrolled diabetes—may further explain why individuals with these conditions are vulnerable to IPD (62, 64, 65). Thus, catabolite repression is possibly a key event in initiating a pathogenic program of *S. pneumoniae*. In support of this notion, a functional CcpA has been determined to be necessary for *S. pneumoniae* virulence (66). Likewise, CCR has been shown to suppress *in vitro* biofilm formation in *E. coli* and *Bacillus subtilis* as well (67, 68).

Along such lines, we determined that a mutant lacking pyruvate oxidase, a critical enzyme in the non-lactic acid fermentation process, was dramatically inhibited for biofilm formation *in vitro* and that biofilm formation could be boosted by the addition of acetate. As indicated, we had previously shown that an *spxB*-deficient mutant did not form biofilms *in vivo* (29). At the time, we attributed this phenotype to impaired autolysis, which has been shown to promote the release of extracellular DNA, due to less H_2O_2 production. We now suggest that *spxB*-deficient pneumococci also fail to form biofilms because they are fundamentally altered in a critical metabolic pathway that feeds into the production of biofilm-required products. Based on our RNA-seq analysis, we now suspect that these biofilm products may include those involved in fatty acid biosynthesis.

A role for fatty acid synthesis and metabolism in *S. pneumoniae* biofilm formation would not be unprecedented. Spo0A, a transcriptional regulator of spore formation in *B. subtilis*, has also been identified as a regulator of *de novo* fatty acid synthesis and was found to be required for biofilm formation. The inability of an Spo0A-deficient mutant to form biofilms *in vitro* was restored by exogenous fatty acid supplementation (69). Likewise, fatty acid kinase A has been shown to be an important determinant of biofilm formation in *Staphylococcus aureus* strain USA300 (70). A recent comparative proteomic study of biofilm and planktonic *Lactococcus plantarum* found that fatty acid metabolism genes were among those with the greatest differential levels during biofilm growth (71). Thus, considerable evidence points to an im-

FIG 6 Metabolic activity of pneumococci during biofilm formation. (A) TIGR4 orthologs of 6A-10 genes determined to be differentially expressed by DESeq analysis of RNA-seq data were subjected to a pathway enrichment analysis performed with GAGE, KEGG orthology terms, and pathway maps for *S. pneumoniae* TIGR4. Heat maps represent the $\log_2$ fold change of biofilm (BF) expression over planktonic (PK) expression. Each subpanel harbors three columns corresponding to the three paired replicates for each condition (3 replicates of BF versus PK). Values of $\log_2$ fold change are indicated for each replicate pair. Compared growth conditions include *S. pneumoniae* strain 6A-10 grown as biofilm in unsupplemented medium (THB BF) or medium supplemented with galactose (GAL BF) versus the planktonic growth phenotype in unsupplemented medium (THB PK) or medium supplemented with glucose (GLU PK) or galactose (GAL PK). Pathways differentially regulated across multiple growth conditions are highlighted with the same background color (e.g., pyruvate metabolism in green). (B) Differentially regulated genes involved in pyruvate metabolism in *S. pneumoniae* were painted on the KEGG pyruvate metabolism reference pathway (SPN00620) using the packages GAGE and Pathview. Each gene/enzyme box is divided into three colored thirds corresponding to the three paired replicates for each condition (3 replicates of THB BF versus THB PK). Differential expression is depicted according to the heat map provided in the upper right corner of panel B. Values are $\log_2$ fold change of biofilm (THB BF) expression over planktonic (THB PK) expression.

portant role for fatty acids during biofilm growth, although it is unclear how fatty acids might specifically contribute to the pneumococcal biofilm phenotype. One obvious possibility is that fatty acids may be part of the extracellular matrix. This is known to be the case for *Candida albicans* and mycobacterial biofilms (72, 73). Alternatively changes in lipid content at the membrane level may facilitate survival in the biofilm, which for the pneumococcus has been postulated to be a stressful environment, as evidenced by the upregulation of heat shock proteins (63). Along such lines, it is worth noting that the protein with the highest level of differential expression in biofilms grown in galactose in our RNA-seq studies was ClpL (SP_0338), a protease and member of the heat shock protein family that is stress regulated (74).

Taken together, our results indicate that carbon availability varies in an anatomical site-specific manner in humans, and this impacts *in vivo* biofilm formation by *S. pneumoniae*. Moreover, we show that neuraminidase A and β-galactosidase A contribute to *in vivo* biofilm formation through the exposure of galactose, a non-CCR-inducing carbon, which ties into biofilm formation through pyruvate- and acetyl coenzyme A (acetyl-CoA) metabolism. While the specific downstream role that fatty acid biosynthesis plays during *S. pneumoniae* biofilm formation remains unclear, the RNA-seq results along with the increasing body of literature that is supportive suggest that this is an important research topic moving forward.

ACKNOWLEDGMENTS

We thank Monica Alarcon and Barbara Hunter for efforts in preparing the mouse nasal septa for scanning electron microscopy. We also thank Norberto Gonzalez-Juarbe for electron microscopy imaging assistance.

This work was supported by National Institutes of Health grants AI078972 and AI114800 to C.J.O. K.A.B. received support through T32DE14318-10 and T32AI7271-24.

The authors of this article have no conflicts of interest.

FUNDING INFORMATION

This work, including the efforts of Carlos J. Orihuela, was funded by HHS | NIH | National Institute of Allergy and Infectious Diseases (NIAID) (AI078972 and AI114800). This work, including the efforts of Krystle A. Blanchette, was funded by HHS | NIH | National Institute of Allergy and Infectious Diseases (NIAID) (T32AI7271-24). This work, including the efforts of Krystle A. Blanchette, was funded by HHS | NIH | National Institute of Dental and Craniofacial Research (NIDCR) (T32DE14318-10).

REFERENCES

1. **Bogaert D, De Groot R, Hermans PW.** 2004. Streptococcus pneumoniae colonisation: the key to pneumococcal disease. Lancet Infect Dis **4:**144–154. http://dx.doi.org/10.1016/S1473-3099(04)00938-7.
2. **Valles J, Diaz E, Martin-Loeches I, Bacelar N, Saludes P, Lema J, Gallego M, Fontanals D, Artigas A.** 2015. Evolution over a 15-year period of the clinical characteristics and outcomes of critically ill patients with severe community-acquired pneumonia. Med Intensiva **40:**238–245. http://dx.doi.org/10.1016/j.medin.2015.07.005.
3. **Black RE, Cousens S, Johnson HL, Lawn JE, Rudan I, Bassani DG, Jha P, Campbell H, Walker CF, Cibulskis R, Eisele T, Liu L, Mathers C, Child Health Epidemiology Reference Group of WHO and UNICEF.** 2010. Global, regional, and national causes of child mortality in 2008: a systematic analysis. Lancet **375:**1969–1987. http://dx.doi.org/10.1016/S0140-6736(10)60549-1.
4. **Hill PC, Cheung YB, Akisanya A, Sankareh K, Lahai G, Greenwood BM, Adegbola RA.** 2008. Nasopharyngeal carriage of Streptococcus pneumoniae in Gambian infants: a longitudinal study. Clin Infect Dis **46:**807–814. http://dx.doi.org/10.1086/528688.
5. **Sleeman KL, Griffiths D, Shackley F, Diggle L, Gupta S, Maiden MC, Moxon ER, Crook DW, Peto TEA.** 2006. Capsular serotype-specific attack rates and duration of carriage of Streptococcus pneumoniae in a population of children. J Infect Dis **194:**682–688. http://dx.doi.org/10.1086/505710.
6. **Crook D, Brueggmann A, Sleeman K, Peto T.** 2004. Pneumococcal carriage. ASM Press, Washington, DC.
7. **World Health Organization.** 2007. Pneumococcal vaccines. WHO position paper. Wkly Epidemiol Rec. **82:**93–104.
8. **Spijkerman J, van Gils EJ, Veenhoven RH, Hak E, Yzerman EP, van der Ende A, Wijmenga-Monsuur AJ, van den Dobbelsteen GP, Sanders EA.** 2011. Carriage of Streptococcus pneumoniae 3 years after start of vaccination program, The Netherlands. Emerg Infect Dis **17:**584–591. http://dx.doi.org/10.3201/eid1704.101115.
9. **Kochanek KD, Xu J, Murphy SL, Minino AM, Kung HC.** 2011. Deaths: preliminary data for 2009. Natl Vital Stat Rep **59:**1–51.
10. **Wunderink RG, Waterer GW.** 2014. Community-acquired pneumonia. N Engl J Med **370:**1863. http://dx.doi.org/10.1056/NEJMc1402692.
11. **Potera C.** 1999. Forging a link between biofilms and disease. Science **283:**1837–1839. http://dx.doi.org/10.1126/science.283.5409.1837.
12. **Costerton J, Stewart P, Greenberg E.** 1999. Bacterial biofilms: a common cause of persistent infections. Science **284:**1318–1322. http://dx.doi.org/10.1126/science.284.5418.1318.
13. **Hall-Stoodley L, Hu FZ, Gieseke A, Nistico L, Nguyen D, Hayes J, Forbes M, Greenberg DP, Dice B, Burrows A, Wackym PA, Stoodley P, Post JC, Ehrlich GD, Kerschner JE.** 2006. Direct detection of bacterial biofilms on the middle-ear mucosa of children with chronic otitis media. JAMA **296:**202–211. http://dx.doi.org/10.1001/jama.296.2.202.
14. **Hoa M, Tomovic S, Nistico L, Hall-Stoodley L, Stoodley P, Sachdeva L, Berk R, Coticchia JM.** 2009. Identification of adenoid biofilms with middle ear pathogens in otitis-prone children utilizing SEM and FISH. Int J Pediatr Otorhinolaryngol **73:**1242–1248. http://dx.doi.org/10.1016/j.ijporl.2009.05.016.
15. **Marks LR, Parameswaran GI, Hakansson AP.** 2012. Pneumococcal interactions with epithelial cells are crucial for optimal biofilm formation and colonization in vitro and in vivo. Infect Immun **80:**2744–2760. http://dx.doi.org/10.1128/IAI.00488-12.
16. **Psaltis AJ, Ha KR, Beule AG, Tan LW, Wormald P-J.** 2007. Confocal scanning laser microscopy evidence of biofilms in patients with chronic rhinosinusitis. Laryngoscope **177:**1302–1306.
17. **Sanclement JA, Webster P, Thomas J, Ramadan HH.** 2005. Bacterial biofilms in surgical specimens of patients with chronic rhinosinusitis. Laryngoscope **115:**578–582. http://dx.doi.org/10.1097/01.mlg.0000161346.30752.18.
18. **Otto M.** 2006. Bacterial evasion of antimicrobial peptides by biofilm formation. Curr Top Microbiol Immunol **306:**251–258.
19. **Fux CA, Costerton JW, Stewart PS, Stoodley P.** 2005. Survival strategies of infectious biofilms. Trends Microbiol **13:**34–40. http://dx.doi.org/10.1016/j.tim.2004.11.010.
20. **Marks LR, Reddinger RM, Hakansson AP.** 2013. Biofilm formation enhances fomite survival of Streptococcus pneumoniae and Streptococcus pyogenes. Infect Immun **82:**1141–1146. http://dx.doi.org/10.1128/IAI.01310-13.
21. **Marks LR, Reddinger RM, Hakansson AP.** 2012. High levels of genetic recombination during nasopharyngeal carriage and biofilm formation in Streptococcus pneumoniae. mBio **3:**e00200-12. http://dx.doi.org/10.1128/mBio.00200-12.
22. **Moscoso M, Garcia E, Lopez R.** 2006. Biofilm formation by Streptococcus pneumoniae: role of choline, extracellular DNA, and capsular polysaccharide in microbial accretion. J Bacteriol **188:**7785–7795. http://dx.doi.org/10.1128/JB.00673-06.
23. **Tettelin H, Nelson KE, Paulsen IT, Eisen JA, Read TD, Peterson S, Heidelberg J, DeBoy RT, Haft DH, Dodson RJ, Durkin AS, Gwinn M, Kolonay JF, Nelson WC, Peterson JD, Umayam LA, White O, Salzberg SL, Lewis MR, Radune D, Holtzapple E, Khouri H, Wolf AM, Utterback TR, Hansen CL, McDonald LA, Feldblyum TV, Angiuoli S, Dickinson T, Hickey EK, Holt IE, Loftus BJ, Yang F, Smith HO, Venter JC, Dougherty BA, Morrison DA, Hollingshead SK, Fraser CM.** 2001. Complete genome sequence of a virulent isolate of Streptococcus pneumoniae. Science **293:**498–506. http://dx.doi.org/10.1126/science.1061217.
24. **Asanuma N, Yoshii T, Hino T.** 2004. Molecular characterization of CcpA and involvement of this protein in transcriptional regulation of lactate dehydrogenase and pyruvate formate-lyase in the ruminal bacterium

Streptococcus bovis. Appl Environ Microbiol **70:**5244–5251. http://dx.doi.org/10.1128/AEM.70.9.5244-5251.2004.
25. **Zheng L, Itzek A, Chen Z, Kreth J.** 2011. Environmental influences on competitive hydrogen peroxide production in Streptococcus gordonii. Appl Environ Microbiol **77:**4318–4328. http://dx.doi.org/10.1128/AEM.00309-11.
26. **Carvalho SM, Kloosterman TG, Kuipers OP, Neves AR.** 2011. CcpA ensures optimal metabolic fitness of Streptococcus pneumoniae. PLoS One **6:**e26707. http://dx.doi.org/10.1371/journal.pone.0026707.
27. **Zheng L, Chen Z, Itzek A, Ashby M, Kreth J.** 2011. Catabolite control protein A controls hydrogen peroxide production and cell death in Streptococcus sanguinis. J Bacteriol **193:**516–526. http://dx.doi.org/10.1128/JB.01131-10.
28. **Spellerberg B, Cundell DR, Sandros J, Pearce BJ, Idanpaan-Heikkila I, Rosenow C, Masure HR.** 1996. Pyruvate oxidase, as a determinant of virulence in Streptococcus pneumoniae. Mol Microbiol **19:**803–813. http://dx.doi.org/10.1046/j.1365-2958.1996.425954.x.
29. **Blanchette-Cain K, Hinojosa CA, Akula Suresh Babu R, Lizcano A, Gonzalez-Juarbe N, Munoz-Almagro C, Sanchez CJ, Bergman MA, Orihuela CJ.** 2013. Streptococcus pneumoniae biofilm formation is strain dependent, multifactorial, and associated with reduced invasiveness and immunoreactivity during colonization. mBio **4:**e00745-13. http://dx.doi.org/10.1128/mBio.00745-13.
30. **Parker D, Soong G, Planet P, Brower J, Ratner AJ, Prince A.** 2009. The NanA neuraminidase of Streptococcus pneumoniae is involved in biofilm formation. Infect Immun **77:**3722–3730. http://dx.doi.org/10.1128/IAI.00228-09.
31. **Trappetti C, Kadioglu A, Carter M, Heyre J, Iannelli F, Pozzi G, Andrew P, Oggioni M.** 2009. Sialic acid: a preventable signal for pneumococcal biofilm formation, colonization, and invasion of the host. J Infect Dis **199:**1497–1505. http://dx.doi.org/10.1086/598483.
32. **Munoz-Elias EJ, Marcano J, Camilli A.** 2008. Isolation of Streptococcus pneumoniae biofilm mutants and their characterization during nasopharyngeal colonization. Infect Immun **76:**5049–5061. http://dx.doi.org/10.1128/IAI.00425-08.
33. **Marion C, Burnaugh AM, Woodiga SA, King SJ.** 2011. Sialic acid transport contributes to pneumococcal colonization. Infect Immun **79:**1262–1269. http://dx.doi.org/10.1128/IAI.00832-10.
34. **Tong HH, Liu X, Chen Y, James M, Demaria T.** 2002. Effect of neuraminidase on receptor-mediated adherence of Streptococcus pneumoniae to chinchilla tracheal epithelium. Acta Otolaryngol **122:**413–419. http://dx.doi.org/10.1080/00016480260000111.
35. **Burnaugh AM, Frantz LJ, King SJ.** 2008. Growth of Streptococcus pneumoniae on human glycoconjugates is dependent upon the sequential activity of bacterial exoglycosidases. J Bacteriol **190:**221–230. http://dx.doi.org/10.1128/JB.01251-07.
36. **King SJ, Hippe KR, Weiser JN.** 2006. Deglycosylation of human glycoconjugates by the sequential activities of exoglycosidases expressed by Streptococcus pneumoniae. Mol Microbiol **59:**961–974. http://dx.doi.org/10.1111/j.1365-2958.2005.04984.x.
37. **Dalia AB, Standish AJ, Weiser JN.** 2010. Three surface exoglycosidases from Streptococcus pneumoniae, NanA, BgaA, and StrH, promote resistance to opsonophagocytic killing by human neutrophils. Infect Immun **78:**2108–2116. http://dx.doi.org/10.1128/IAI.01125-09.
38. **Ferreira DM, Neill DR, Bangert M, Gritzfeld JF, Green N, Wright AK, Pennington SH, Bricio-Moreno L, Moreno AT, Miyaji EN, Wright AD, Collins AM, Goldblatt D, Kadioglu A, Gordon SB.** 2013. Controlled human infection and rechallenge with Streptococcus pneumoniae reveals the protective efficacy of carriage in healthy adults. Am J Respir Crit Care Med **187:**855–864. http://dx.doi.org/10.1164/rccm.201212-2277OC.
39. **Glennie S, Gritzfeld JF, Pennington SH, Garner-Jones M, Coombes N, Hopkins MJ, Vadesilho CF, Miyaji EN, Wang D, Wright AD, Collins AM, Gordon SB, Ferreira DM.** 2016. Modulation of nasopharyngeal innate defenses by viral coinfection predisposes individuals to experimental pneumococcal carriage. Mucosal Immunol **9:**56–67. http://dx.doi.org/10.1038/mi.2015.35.
40. **Gritzfeld JF, Wright AD, Collins AM, Pennington SH, Wright AK, Kadioglu A, Ferreira DM, Gordon SB.** 2013. Experimental human pneumococcal carriage. J Vis Exp http://dx.doi.org/10.3791/50115.
41. **National Research Council.** 2011. Guide for the care and use of laboratory animals, 8th ed. National Academies Press, Washington, DC.
42. **Lanie JA, Ng WL, Kazmierczak KM, Andrzejewski TM, Davidsen TM, Wayne KJ, Tettelin H, Glass JI, Winkler ME.** 2007. Genome sequence of Avery's virulent serotype 2 strain D39 of Streptococcus pneumoniae and comparison with that of unencapsulated laboratory strain R6. J Bacteriol **189:**38–51. http://dx.doi.org/10.1128/JB.01148-06.
43. **Embry A, Hinojosa E, Orihuela C.** 2007. Regions of diversity 8, 9 and 13 contribute to Streptococcus pneumoniae virulence. BMC Microbiol **7:**80.
44. **Haas W, Sublett J, Kaushai D, Tuonmanen E.** 2004. Revising the role of the pneumococcal vex-vncRS locus in vancomycin tolerance. J Bacteriol **186:**8463–8471. http://dx.doi.org/10.1128/JB.186.24.8463-8471.2004.
45. **Antunes MB, Woodworth BA, Bhargave G, Xiong G, Aguilar JL, Ratner AJ, Kreindler JL, Rubenstein RC, Cohen NA.** 2007. Murine nasal septa for respiratory epithelial air-liquid interface cultures. Biotechniques **43:**195–204. http://dx.doi.org/10.2144/000112531.
46. **Langmead B, Trapnell C, Pop M, Salzberg SL.** 2009. Ultrafast and memory-efficient alignment of short DNA sequences to the human genome. Genome Biol **10:**R25. http://dx.doi.org/10.1186/gb-2009-10-3-r25.
47. **Anders S, Pyl PT, Huber W.** 2015. HTSeq—a Python framework to work with high-throughput sequencing data. Bioinformatics **31:**166–169. http://dx.doi.org/10.1093/bioinformatics/btu638.
48. **Anders S, Huber W.** 2010. Differential expression analysis for sequence count data. Genome Biol **11:**R106. http://dx.doi.org/10.1186/gb-2010-11-10-r106.
49. **Luo W, Friedman MS, Shedden K, Hankenson KD, Woolf PJ.** 2009. GAGE: generally applicable gene set enrichment for pathway analysis. BMC Bioinformatics **10:**161. http://dx.doi.org/10.1186/1471-2105-10-161.
50. **Kanehisa M, Goto S.** 2000. KEGG: Kyoto Encyclopedia of Genes and Genomes. Nucleic Acids Res **28:**27–30. http://dx.doi.org/10.1093/nar/28.1.27.
51. **Luo W, Brouwer C.** 2013. Pathview: an R/Bioconductor package for pathway-based data integration and visualization. Bioinformatics **29:**1830–1831. http://dx.doi.org/10.1093/bioinformatics/btt285.
52. **Buckwalter CM, King SJ.** 2012. Pneumococcal carbohydrate transport-food for thought. Trends Microbiol **20:**517–522. http://dx.doi.org/10.1016/j.tim.2012.08.008.
53. **Gualdi L, Hayre JK, Gerlini A, Bidossi A, Colomba L, Trappetti C, Pozzi G, Docquier JD, Andrew P, Ricci S, Oggioni MR.** 2012. Regulation of neuraminidase expression in Streptococcus pneumoniae. BMC Microbiol **12:**200. http://dx.doi.org/10.1186/1471-2180-12-200.
54. **King SJ, Whatmore AM, Dowson CG.** 2005. NanA, a neuraminidase from Streptococcus pneumoniae, shows high levels of sequence diversity, at least in part through recombination with Streptococcus oralis. J Bacteriol **187:**5376–5386. http://dx.doi.org/10.1128/JB.187.15.5376-5386.2005.
55. **Afzal M, Shafeeq S, Ahmed H, Kuipers OP.** 2015. Sialic acid-mediated gene expression in Streptococcus pneumoniae and role of NanR as a transcriptional activator of the nan gene cluster. Appl Environ Microbiol **81:**3121–3131. http://dx.doi.org/10.1128/AEM.00499-15.
56. **Marion C, Aten AE, Woodiga SA, King SJ.** 2011. Identification of an ATPase, MsmK, which energizes multiple carbohydrate ABC transporters in Streptococcus pneumoniae. Infect Immun **79:**4193–4200. http://dx.doi.org/10.1128/IAI.05290-11.
57. **Tong HH, Li D, Chen S, Long JP, DeMaria TF.** 2005. Immunization with recombinant Streptococcus pneumoniae neuraminidase NanA protects chinchillas against nasopharyngeal colonization. Infect Immun **73:**7775–7778. http://dx.doi.org/10.1128/IAI.73.11.7775-7778.2005.
58. **Tong HH, Blue LE, James MA, DeMaria TF.** 2000. Evaluation of the virulence of a Streptococcus pneumoniae neuraminidase-deficient mutant in nasopharyngeal colonization and development of otitis media in the chinchilla model. Infect Immun **68:**921–924. http://dx.doi.org/10.1128/IAI.68.2.921-924.2000.
59. **Brittan JL, Buckeridge TJ, Finn A, Kadioglu A, Jenkinson HF.** 2012. Pneumococcal neuraminidase A: an essential upper airway colonization factor for Streptococcus pneumoniae. Mol Oral Microbiol **27:**270–283. http://dx.doi.org/10.1111/j.2041-1014.2012.00658.x.
60. **Limoli DH, Sladek JA, Fuller LA, Singh AK, King SJ.** 2011. BgaA acts as an adhesin to mediate attachment of some pneumococcal strains to human epithelial cells. Microbiology **157:**2369–2381. http://dx.doi.org/10.1099/mic.0.045609-0.
61. **Sanchez CJ, Hinojosa CA, Shivshankar P, Hyams C, Camberlein E, Brown JS, Orihuela CJ.** 2011. Changes in capsular serotype alter the surface exposure of pneumococcal adhesins and impact virulence. PLoS One **6:**e26587. http://dx.doi.org/10.1371/journal.pone.0026587.
62. **Marks LR, Davidson BA, Knight PR, Hakansson AP.** 2013. Interking-

dom signaling induces Streptococcus pneumoniae biofilm dispersion and transition from asymptomatic colonization to disease. mBio **4:**e00438-13. http://dx.doi.org/10.1128/mBio.00438-13.
63. **Sanchez CJ, Kumar N, Lizcano A, Shivshankar P, Dunning Hotopp JC, Jorgensen JH, Tettelin H, Orihuela CJ.** 2011. Streptococcus pneumoniae in biofilms are unable to cause invasive disease due to altered virulence determinant production. PLoS One **6:**e28738. http://dx.doi.org/10.1371/journal.pone.0028738.
64. **Mathews CE, Brown EL, Martinez PJ, Bagaria U, Nahm MH, Burton RL, Fisher-Hoch SP, McCormick JB, Mirza S.** 2012. Impaired function of antibodies to pneumococcal surface protein A but not to capsular polysaccharide in Mexican American adults with type 2 diabetes mellitus. Clin Vaccine Immunol **19:**1360–1369. http://dx.doi.org/10.1128/CVI.00268-12.
65. **Almeida ST, Nunes S, Santos Paulo AC, Valadares I, Martins S, Breia F, Brito-Avo A, Morais A, de Lencastre H, Sa-Leao R.** 2014. Low prevalence of pneumococcal carriage and high serotype and genotype diversity among adults over 60 years of age living in Portugal. PLoS One **9:**e90974. http://dx.doi.org/10.1371/journal.pone.0090974.
66. **Iyer R, Baliga NS, Camilli A.** 2005. Catabolite control protein A (CcpA) contributes to virulence and regulation of sugar metabolism in Streptococcus pneumoniae. J Bacteriol **187:**8340–8349. http://dx.doi.org/10.1128/JB.187.24.8340-8349.2005.
67. **Jackson DW, Simecka JW, Romeo T.** 2002. Catabolite repression of Escherichia coli biofilm formation. J Bacteriol **184:**3406–3410. http://dx.doi.org/10.1128/JB.184.12.3406-3410.2002.
68. **Stanley NR, Britton RA, Grossman AD, Lazazzera BA.** 2003. Identification of catabolite repression as a physiological regulator of biofilm formation by Bacillus subtilis by use of DNA microarrays. J Bacteriol **185:**1951–1957. http://dx.doi.org/10.1128/JB.185.6.1951-1957.2003.
69. **Pedrido ME, de Ona P, Ramirez W, Lenini C, Goni A, Grau R.** 2013. Spo0A links de novo fatty acid synthesis to sporulation and biofilm development in Bacillus subtilis. Mol Microbiol **87:**348–367. http://dx.doi.org/10.1111/mmi.12102.
70. **Sabirova JS, Hernalsteens JP, De Backer S, Xavier BB, Moons P, Turlej-Rogacka A, De Greve H, Goossens H, Malhotra-Kumar S.** 2015. Fatty acid kinase A is an important determinant of biofilm formation in Staphylococcus aureus USA300. BMC Genomics **16:**861. http://dx.doi.org/10.1186/s12864-015-1956-8.
71. **De Angelis M, Siragusa S, Campanella D, Di Cagno R, Gobbetti M.** 2015. Comparative proteomic analysis of biofilm and planktonic cells of Lactobacillus plantarum DB200. Proteomics **15:**2244–2257. http://dx.doi.org/10.1002/pmic.201400363.
72. **Lopez-Ribot JL.** 2014. Large-scale biochemical profiling of the Candida albicans biofilm matrix: new compositional, structural, and functional insights. mBio **5:**e01781-14.
73. **Zambrano MM, Kolter R.** 2005. Mycobacterial biofilms: a greasy way to hold it together. Cell **123:**762–764. http://dx.doi.org/10.1016/j.cell.2005.11.011.
74. **Park SS, Kwon HY, Tran TD, Choi MH, Jung SH, Lee S, Briles DE, Rhee DK.** 2015. ClpL is a chaperone without auxiliary factors. FEBS J **282:**1352–1367. http://dx.doi.org/10.1111/febs.13228.